Time-domain PEEC Transient Analysis for a Wire Structure above Perfectly-conducting Ground with the Incident Field from a Distant Lightning Channel

Ruihan Qi, Y. Du[1] and Mingli Chen

The Hong Kong Polytechnic University, Dept. of Building Services Engineering,

Hung Hom, Kowloon, Hong Kong

[1]ya-ping.du@polyu.edu.hk

Abstract —**This paper presents the time-domain PEEC analysis of induced transients in a wire structure during an indirect lightning strike. The full-wave PEEC formulation with an external incident field is employed. The incident field is calculated with either the Uman's or the Jefimenko's formula by using the engineering model of a lightning channel. An instability problem is, however, observed. It becomes a hurdle in the application of PEEC for evaluating induced transient currents in closed wire loops. The problem is investigated, and is primarily caused by discretization of electric field in numerical evaluation of external voltage source. An improved algorithm is provided to solve this instability problem, and is tested in both near and far field zones. It is validated by the FDTD method. The issue of time step and segment length is addressed. It is also found that the Uman's formula is generally incapable of producing stable induced currents in a wire-loop structure. Finally the proposed PEEC procedure is applied to evaluate induced lightning transients in a PV panel during an indirect lightning strike.**

Keywords — **lightning, induced transient, wire and PEEC**

I. Introduction

Nowadays, electronic and electrical equipment continues to proliferate to meet the ever-increasing demand of businesses. It is quite common for wiring systems with lengths of up to tens of meters to be provided for device connection and others. These lines may not be struck by lightning directly, but can be subject to lightning transients during indirect lightning strikes. The equipment connected would be damaged or malfunction if protection is not provided appropriately. It is therefore necessary to provide an effective approach for the evaluation of lightning induced transients in such wiring systems.

In past decades, transmission line (TL) transients have been studies extensively in an indirect lightning strike. Several field-to-transmission line coupling models have been provided to analyze induced lightning transients [1-4]. In these models, the incident field was calculated with the Uman's formula by using the engineering models of a lightning return stroke [5]. It was found [6-7] that the Agrawal model [2] was the simplest and accurate coupling model for studying lightning induced effects. For a finite-length line the theory and fast iterative numerical solution of induced lightning transients were studied as well [8]. The coupling equations with some additional source terms representing the correction to the TL approximation were presented. However, induced transients in an arbitrary (closed) wire structures during an indirect lightning strike has not been addressed significantly in the literature.

Lightning transients in a wire structure during a direct lightning strike have been well studied. In [9-10] transients in an overhead line connected to a tower were analyzed using the partial element equivalent circuit (PEEC) method. In [11-13] the PEEC model for the lightning protection system and/or the braided coaxial cables was proposed for the analysis of transients during a lightning strike. In [14-15] lightning transient currents in radio base stations were analyzed by using the PEEC method. Cables, structural steels wires and grounding grids were represented with circuit components.

Lightning transients in a line structure can be also evaluated using other numerical methods, such as finite-difference-time-domain (FDTD) [16-18] and finite element method (FEM) [19]. These methods can deal with complex geometry and the material characteristics of conductive bodies. Note that they need to discretize the whole problem domain into a large number of small cells. For the delicate wire structure, the cell length needs to be small enough to ensure realistic results. As a result, both memory space and computation time increase significantly, compared with the PEEC and TL methods which need to model the conductors only.

This paper addresses the full-wave PEEC formulation of a wire structure, particularly with closed loops, for induced transient analysis under the excitation from a distant lightning channel. The perfectly conducting ground is considered in this paper. Similar to the field-to-line model, the external incident field source is calculated by using the engineering model of a lighting channel. An instability problem was encountered when evaluating induced lightning transient currents in a closed loop. This instability problem is investigated in Section III, and its root cause is discussed. An improved algorithm is provided for stable induced transient current evaluation, and a comparison with the FDTD method is presented. Discussion on using the Uman's formula for calculating external voltage source is presented as well. Finally, the proposed PEEC formulation with the improved algorithm for the incident source voltage is applied to evaluate induced lightning transients in the DC power circuit of a PV panel during an indirect lightning strike.

II. PEEC Formulation for Induced Lightning Transient Analysis

The PEEC method is widely used for modeling 3D interconnected thin-wire structure with retardation effect [20]. It is derived from a mixed potential integral equation, and transforms an electromagnetic field problem into the circuit domain. Both voltage and current in the wire structure can be solved directly using a conventional circuit analysis tool.

A) General PEEC equations

The general PEEC equation is obtained from the following boundary equation enforced on the surface of a wire,

$$\hat{n}\times \boldsymbol{E}^{i}(r)+\hat{n}\times \boldsymbol{E}^{s}(r)=\hat{n}\times \boldsymbol{E}^{T}(r) \tag{1}$$

where $\hat{n}$ is a surface normal. Both $\boldsymbol{E}^{i}$ and $\boldsymbol{E}^{T}$ are respectively the independent incident electric field and the electric field on the conductor surface. $\boldsymbol{E}^{s}$ is the scattered electric field. It can be expressed using electric scalar potential ϕ and magnetic vector potential A in the frequency domain as

$$\boldsymbol{E}^{s}(r)=-j\omega \boldsymbol{A}(r)-\nabla\phi(r) \tag{2}$$

Now consider wires in air above perfectly conducting ground. Both ϕ and $\boldsymbol{A}$ can be expressed with charge density λ and current I in the wires [21] using Green's functions, as follows:

$$\begin{aligned}\boldsymbol{A}(r)&=\frac{\mu_0}{4\pi}\left[\int_{l'}G_0(r,r')\boldsymbol{I}(r')d\boldsymbol{l}'-\int_{l''}\overline{\overline{G}}_A(r,r'')\boldsymbol{I}(r'')\cdot d\boldsymbol{l}''\right]\\ \phi(r)&=\frac{1}{4\pi\varepsilon_0}\left[\int_{l'}G_0(r,r')\lambda(r')dl'-\int_{l''}G_0(r,r'')\lambda(r'')dl''\right]\end{aligned} \tag{3}$$

where Green's function $G_0(r,r^*)=e^{-jk_0|r-r^*|}/|r-r^*|$ ($r^*=r'$ or r'') with wave number $k_0=\omega\sqrt{\mu_0\epsilon_0}$. Dyadic Green's function $\overline{\overline{G}}_A=G_0(r,r'')(\hat{\rho}\hat{\rho}-\hat{z}\hat{z})$. Both $\hat{\rho}$ and $\hat{z}$ are respectively the unit vectors in parallel with and perpendicular to the ground plane, as shown in Fig. 1. Both l' and l'' are the source wire and its mirror image with respect to the ground plane. Tangential surface electric field $\hat{n}\times\boldsymbol{E}^{T}$ in (1) can be expressed using surface impedance of a wire. For a cylindrical wire of radius r_a, it is given by

$$\begin{aligned}&\hat{n}\times\boldsymbol{E}^{t}=Z_s(\omega)\boldsymbol{I}\\ &Z_s(\omega)=\frac{j\omega\mu}{2\pi R_a}\cdot\frac{I_0(R_a)}{I_1(R_a)}\end{aligned} \tag{4}$$

where $R_a=\sqrt{j\omega\mu\sigma}r_a$, and I_n are modified Bessel functions of the 1st kind with order *n*.

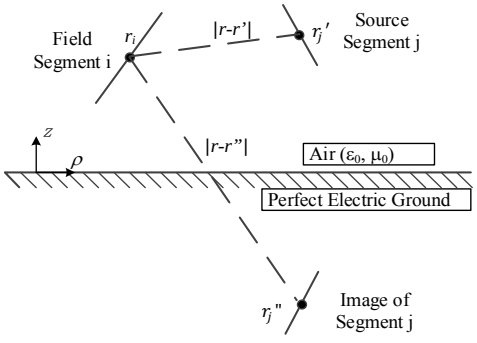

Fig. 1 Configuration of segments in the air-ground media

Divide the wires into a number of segments and assume both current and charge density in each segment are constant. Integrating (1) along segment i then yields a circuit equation for branch current I and node charge q, as follows:

$$\begin{aligned}\phi_n-\phi_{n+1}&=V_i+\sum\nolimits_j(L_{ij,a}-L_{ij,g})\frac{dI_i(t-\tau_{ij})}{dt}+\int_{l_i}\boldsymbol{E}^{i}\cdot d\boldsymbol{l}\\ \phi_n&=\sum\nolimits_k(p_{nm,a}-p_{nm,g})q_m(t-\tau_{ij})\Delta l_m\end{aligned} \tag{5}$$

where time delay $\tau_{ij}=|r_i-r_j'|/c$ (c is the speed of light) between centers of two segments. Circuit parameters $L_{ij,a}$ and $p_{ij,a}$ for source wires in air and $L_{ij,g}$ and $p_{ij,g}$ for their images under the ground are given by

$$L_{ij,a}=\frac{\mu_0}{4\pi}\int_{l_i}\int_{l_j'}\frac{1}{|r-r'|}d\boldsymbol{l}_i\cdot d\boldsymbol{l}_j'$$

$$p_{nm,a}=\frac{1}{4\pi\varepsilon_0}\frac{1}{l_n l_m}\int_{l_n}\int_{l_m'}\frac{1}{|r-r''|}dl_n dl_m'$$

$$L_{ij,g}=\frac{\mu_0}{4\pi}\int_{l_i}\int_{l_j''}\frac{1}{|r-r''|}(\hat{\rho}\hat{\rho}-\hat{z}\hat{z})d\boldsymbol{l}_i d\boldsymbol{l}_j''$$

$$p_{nm,g}=\frac{1}{4\pi\varepsilon_0}\frac{1}{\Delta l_n\Delta l_m}\int_{l_n}\int_{l_m''}\frac{1}{|r-r''|}dl_n dl_m''$$

Both Δl_n and Δl_m are the lengths of the source and field segments. V_i in (5) is the voltage response of wire current associated with frequency-variant surface impedance Z_s. Note that Z_s in s domain can be approximated by rational functions with a vector fitting technique [22], as follows:

$$Z_s(s)=R_0+sL_0+\sum_{i=1}^{N}\frac{s}{s+R_i/L_i}\cdot R_i \tag{6}$$

This rational function is implemented with a sub-circuit $\mathscr{N}$ consisting of series RL circuits, as shown in Fig. 2(a). The complete equivalent circuit including the surface impedance of the segment is given in Fig. 2(b).

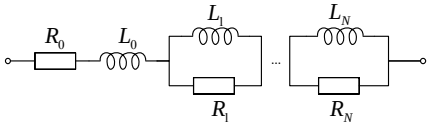

(a) Equivalent circuit of surface impedance $Z_s(\omega)$

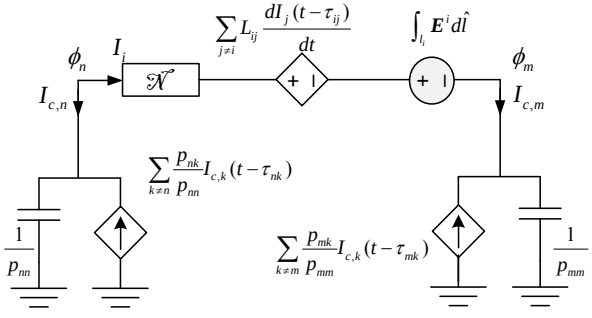

(b) Equivalent circuit with an external incident field

Fig. 2 Equivalent circuit of a line segment

B) Incident electric field from a lightning channel

In a distant lightning flash, the return stroke current is not affected by the ground structure of concern. The electric field

generated from a lightning channel is then considered as an independent external incident field. Although the lightning flash is a random event, a pre-defined current in the lightning channel is always adopted in the evaluation of induced transients in the ground structure.

Engineering models of the lightning return stroke are commonly used to address lightning–generated electromagnetic phenomena. In these models the spatial distribution and temporal variation of the current $I(z',t)$ in the lightning channel are described with an analytical formula, using the channel base current, as follows [23],

$$I(z',t) = u(t - z'/v_f)\, p(z') I(0, t - z'/v) \tag{7}$$

where Heaviside function $u(t)$ is equal to unity for $t > z'/v_f$, and is zero otherwise. $p(z')$ is the height-dependent current attenuation factor introduced in [24]. Both v_f and v are the return-stroke speed and the current-wave propagation speed.

Electromagnetic fields generated in a lightning flash are commonly calculated using the Uman's formula [25-26], especially in the evaluation of induced transients on overhead lines. Consider a vertical straight lightning channel along the z axis above the perfectly conducting ground. The time-domain expression of E field for dz' in the spherical coordinate system with unit vectors $\hat{r}$, $\hat{\theta}$ and $\hat{\varphi}$ is given by

$$d\boldsymbol{E}^i(r,t) = \frac{1}{4\pi\varepsilon_0}\left(\int_0^t \frac{I(z',\tau')\left[2\cos\theta\,\hat{r} + \sin\theta\,\hat{\theta}\right]}{R^3} d\tau + \frac{I(z',t')\left[2\cos\theta\,\hat{r} + \sin\theta\,\hat{\theta}\right]}{cR^2} + \frac{\partial I(z',t')}{c^2 R\,\partial t'} \sin\theta\,\hat{\theta} \right) dz' \tag{8}$$

where $t' = t - R/c$, $\tau' = \tau - R/c$, and $R = \sqrt{\rho^2 + (z - z')^2}$.

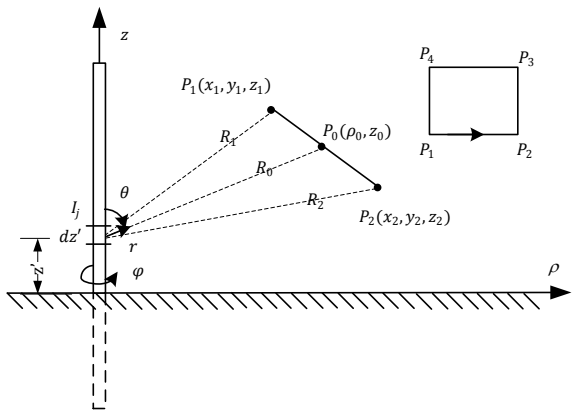

Fig. 3 configuration of a lightning channel and a field point/line

The lightning-generated electric field can be evaluated by using the Jefimenko's formula as well [25-26]. This formula is derived directly from an auxiliary potential equation similar to (2). It is expressed as,

$$d\boldsymbol{E}^i(r,t) = \frac{1}{4\pi\varepsilon_0}\left[\frac{q(z',t')}{R^2}\hat{r} + \frac{\partial q(z',t')}{cR\,\partial t'}\hat{r} - \frac{\partial I(z',t')}{c^2 R\,\partial t'}\hat{z} \right] dz' \tag{9}$$

Although (8) and (9) look different, these expressions are essentially the same as they are all derived from the same auxiliary potential equation. Fig. 3 shows electric fields evaluated at the height of 2 m above the ground with the distance of 100 m and 1000 m from a vertical lightning channel. The channel base current has the waveform of 0.25/100 μs and the magnitude of 10 kA. It is assumed that $p(z') = e^{-z'/1700}$, and $v_f = v = 1.1 \times 10^8$ m/s. It is found that the error of the electric field calculated by two formulas is less than 1% in both cases.

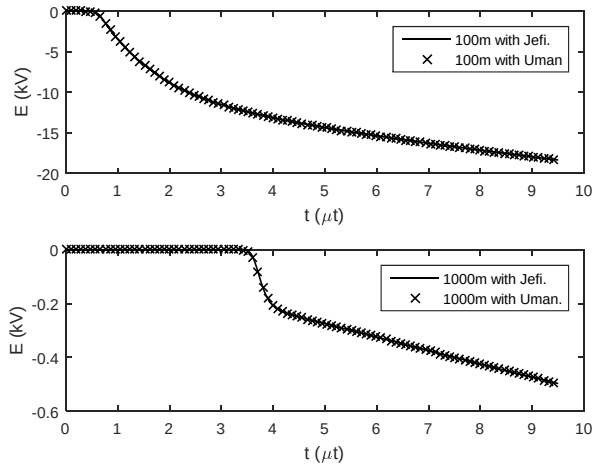

Fig. 3 Electric fields calculated with Uman's and Jefimenko's formulas

C) Time-domain PEEC simulation equations

With (5), matrix equations for $\boldsymbol{\phi}_\mathbf{n}$ and $\mathbf{I_b}$ in the wire structure excited by a lightning channel can be established as,

$$\begin{aligned} \mathbf{A}\boldsymbol{\Phi}_\mathbf{n}(t) &= \mathbf{R}\mathbf{I}_\mathbf{b}(t) + \mathbf{L}_\mathbf{a}\frac{d\mathbf{I}_\mathbf{b}(t-\tau)}{dt} + \mathbf{L}_\mathbf{g}\frac{d\mathbf{I}_\mathbf{b}(t-\tau)}{dt} + \mathbf{v}_\mathbf{s}(t) \\ \boldsymbol{\Phi}_\mathbf{n}(t) &= \mathbf{P}_\mathbf{a}\mathbf{q}(t-\tau) + \mathbf{P}_\mathbf{g}\,\mathbf{q}(t-\tau) \end{aligned} \tag{10}$$

where $\mathbf{v_s}$ is the vectors for external incident field source. $\mathbf{R}$, $\mathbf{L_a}$, $\mathbf{L_g}$, $\mathbf{P_a}$ and $\mathbf{P_g}$ are the circuit parameter matrices.

Now consider the retardation effect in (10). Decouple parameter matrices $\mathbf{L_a}$ and $\mathbf{P_a}$ into two sets of full matrices: (i) $\mathbf{L_s}$ and $\mathbf{P_s}$ in which all entries with non-zero time delay are replaced by zeros, and (ii) $\mathbf{L_m}$ and $\mathbf{P_m}$ in which all entries with zero time delay are replaced by zeros. Note that both $\mathbf{L}_s$ and $\mathbf{P}_s$ may not be the diagonal matrices. Let capacitive current $\mathbf{I_c} = d\mathbf{q}(t)/dt$. The following equation is then obtained from (10),

$$\frac{d\boldsymbol{\Phi}_n(t)}{dt} = \mathbf{P}\mathbf{I}_\mathbf{c}(t) + \mathbf{P}_\mathbf{m}\mathbf{I}_\mathbf{c}(t-\tau_a) + \mathbf{P}_\mathbf{g}\mathbf{I}_\mathbf{c}(t-\tau_g) \tag{11}$$

where τ_a and τ_g are the time delay for the elements above and below the ground plane, respectively.

A set of matrix circuit equations for the wire structure are then established as follows,

$$\begin{bmatrix} -\mathbf{A} & -\mathbf{R} - \dfrac{\mathbf{L_s}}{T} \\ \dfrac{\mathbf{P_s^{-1}}}{T} & -\mathbf{A}^\mathbf{T} \end{bmatrix} \begin{bmatrix} \boldsymbol{\Phi}_\mathbf{n}[n] \\ \mathbf{I_b}[n] \end{bmatrix} = \begin{bmatrix} \dfrac{\mathbf{L_m}}{T}(\mathbf{I_b}[n-m_a-1] - \mathbf{I_b}[n-m_a]) \\ \mathbf{P_s^{-1}}\mathbf{P_m}\mathbf{I_c}[n-m_a] \end{bmatrix}$$

$$+\frac{\mathbf{L_g}}{T}(\mathbf{I_b}[n-m_g-1]-\mathbf{I_b}[n-m_g])-\frac{\mathbf{L_s}}{T}\mathbf{I_b}[n-1]+\mathbf{v_s}[n]$$
$$+\frac{\mathbf{P_s^{-1}}}{T}\mathbf{\Phi_n}[n-1]+\mathbf{P_s^{-1}P_g}\mathbf{I_c}[n-m_g]\Big] \quad (12)$$
$$\mathbf{I_c}[n]=\mathbf{P_s^{-1}}/T\,(\mathbf{\Phi_n}[n]-\mathbf{\Phi_n}[n-1])-$$
$$\mathbf{P_s^{-1}P_m}\mathbf{I_c}[n-m_g]-\mathbf{P_s^{-1}P_m}\mathbf{I_c}[n-m_g]$$

where m_a and m_g denote the discrete time delay for segments above and below the ground, respectively.

III. Instability Problem and Improved Algorithm

A) *Unbounded induced current in a closed loop*

The procedure presented in Section II has been applied to evaluate induced transients during an indirect lightning strike. It was found that the lightning current in a wire structure with closed loops might not be stable.

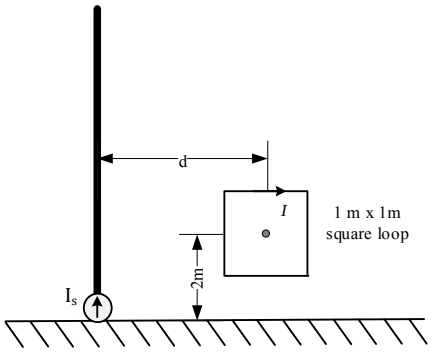

Fig. 4 Configuration for instability problem investigation

Fig. 4 shows the configuration of a system for the illustration of this instability problem. A vertical lightning channel is excited by a channel base impulse current. Channel base current I_s has the waveform of 0.25/100 μs and the amplitude of 10 kA. One square loop of 1 m x 1 m with the wire radius of 10 mm is placed at the distance of d to the channel. In the PEEC simulation, the wires in the square loop are divided into segments with the length of 0.1 m. The time step is 1.9 ns.

In the PEEC model the current in a lightning channel is determined by the engineering model, and calculated with (7). The external field source resulting from the lightning channel current is calculated with either the Uman's formula in (8) or the Jefimenko's formula in (9). A 10-point Gauss-Legendre integration technique is applied to calculate the line integral of the incident electric field, as required in (5). Fig. 5 shows the simulation results of the induced current in the loop with $d =$ 10 m. The normalized channel base current is presented in the figure as well for comparison. It is clearly seen that the induced current calculated with the PEEC approach increases continuously. This indicates that the existing PEEC approach has the difficulty in the evaluation of lightning transients in a closed wire structure.

The external source voltage in the closed loop was evaluated as well. Fig. 6 shows the source loop voltage calculated with the Uman's and Jefimenko's formulas. It is observed that total loop voltage e_s is not trivial even if the lightning channel current changes slowly in its tail in both cases. By ignoring the wire resistance induced loop current i_{loop} at the wave tail can be estimated approximately by,

$$i_{loop}(t)=\frac{1}{L}\int_0^t e_s(\tau)d\tau\,, \quad (13)$$

where L is the loop inductance. It is clearly seen that the induced current will grow to infinity if the source voltage keeps positive or negative. This is the primary reason for the unbounded induced current in a wire loop observed in Fig.5.

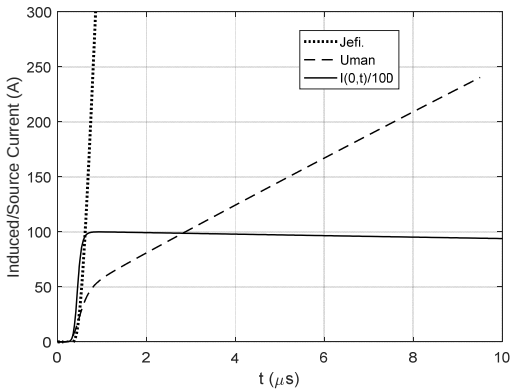

Fig. 5 Instability problem of the incident field calculated with (8) or (9)

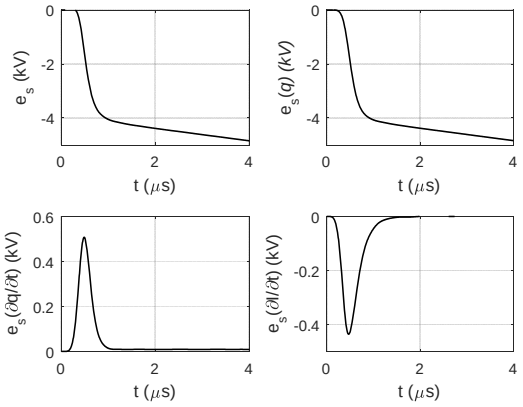

(a) Contribution of $q, dq/dt$ and dI/dt in the Jefimenko's formula

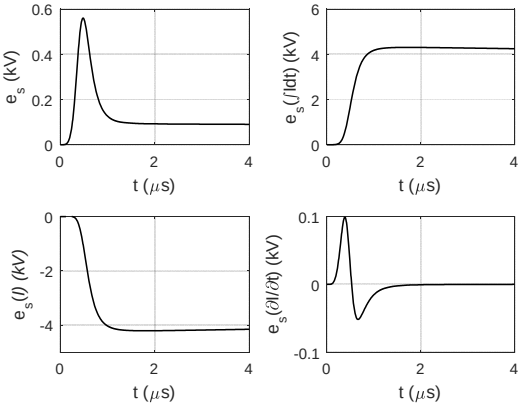

(b) Contribution of $\int Id\tau, I$ and dI/dt in the Uman's formula

Fig. 6 Source loop voltages contributed by three items in (8) and (9)

B) *Improved algorithm for the Jefimenko's formula*

Fig. 6(a) also shows components of the source loop voltage contributed by three items in the Jefimenko's formula: charge,

time derivative of charge and time derivative of current. It is found that the 1st component is significantly large even if the lightning current changes slowly with time at the tail. It is known that the source loop voltage can be theoretically evaluated by taking the closed-contour integration of electric field given in (9), as follows:

$$e_s = \int_C \boldsymbol{E}_{jefi} \cdot d\boldsymbol{l}' = \iint_S \nabla \times \boldsymbol{E}_{jefi} \cdot d\boldsymbol{S}$$
$$= -\frac{1}{4\pi\varepsilon_0} \iint_S \frac{\sin\theta}{c^3 R}\left[\frac{c}{R}\frac{\partial I(z',t')}{\partial t'} + \frac{\partial^2 I(z',t')}{\partial t'^2}\right]\hat{\varphi} \cdot d\boldsymbol{S} \quad (14)$$

The identity of $\partial I(z',t')/\partial R = -1/c\,\partial I(z',t')/\partial t'$ was employed in deriving (14).

It is known in (14) that the source loop voltage is determined by the time-derivative of current. The components contributed by charge and its derivative are found to be zero. It is then reasonable to state that the non-trivial voltage components in Fig. 6(a) are caused by the discretization of electric field in their numerical evaluation. The errors introduced in the evaluation of segment source voltage cannot be cancelled out in the determination of source loop voltage. The numerical integration technique can improve the accuracy of the external source in each segment. It is, however, not enough to retain sufficient accuracy when the cancellation effect of the voltages from several segments in a loop is significant.

Note that electric field contributed by charge is conservative. An analytical formula of external source voltage can be derived by taking a line integral of electric field in (9) along field segment L_i. Numerical integration of E field arising from charge is then avoided. In this case, the lightning channel is divided into a number of segments. Each segment is treated as a point source. For source segment z_i with the length of Δz_i as show in Fig. 1, the source voltage on L_i is expressed by

$$v_{s,ij} = \frac{1}{4\pi\varepsilon_0}\left[\frac{q_j(\tau_1)_i}{R_1} - \frac{q_j(\tau_2)}{R_2} + \ln\frac{a+R_1}{a+\Delta L_i + \sqrt{(a+\Delta L_i)^2 - a^2 + R_1^2}}\frac{\partial I_j(\tau_0)}{c^2\,\partial\tau}\Delta l_j \cos\gamma\right] \quad (15)$$

where $a = x_1 cos\alpha + y cos\beta + z_1 cos\gamma$, and $cos\alpha$, $cos\beta$ and $cos\gamma$ are the directional numbers of the field segment. Both $q(\tau_k)$ and $I(\tau_k)$ are retarded charge and current with $\tau_k = t - R_k/c$ ($k = 0, 1$ and 2). R_0, R_1 and R_2 are the distances from the source point to the middle point and two ends of the field segment. In case of a closed field loop as shown in Fig.1, the source loop voltage contributed by the charge is identical to zero as its E field is conservative. According to (15), the phenomenon of the unbounded induced current arising from the charge in source segments disappears.

Fig. 8 shows the comparison of induced current in a 1 m x 1 m square loop calculated by FDTD and PEEC methods. The configuration of the testing system is illustrated in Fig. 4. The external incident field is generated by a monopole fed by a current source connected at the ground. The distance between the loop and the antenna is equal to 10 m. As a first step, FDTD is applied to calculate both the induced current in the loop and the current in the antenna. The antenna current is then used to calculate external source voltage in each wire segment with the revised formula given in (15) for PEEC simulation. The time steps in PEEC and FDTD simulations were set to 1.9 ns and 0.19 ns, respectively. It is found in Fig. 8 that the induced current obtained in the PEEC simulation is stable, and matches with the FDTD result very well. The difference of the current at its tail is less than 1% generally.

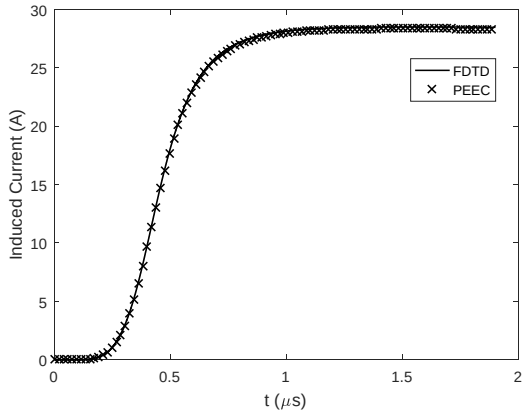

Fig. 8 Comparison of induced loop current calculated by FDTD and PEEC

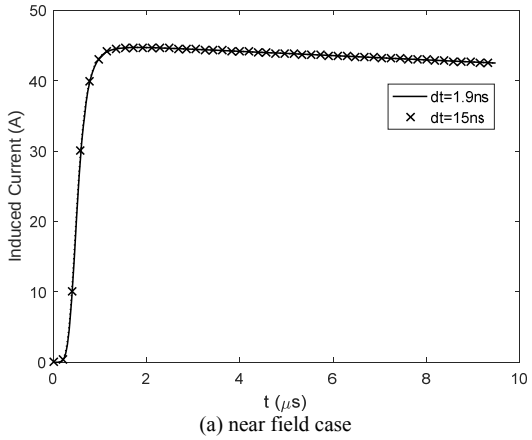

(a) near field case

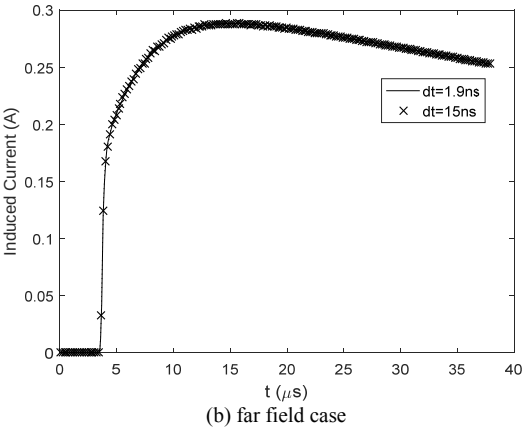

(b) far field case

Fig. 9 Induced loop current calculated with (17) during a lighting strike

Fig. 9 shows the induced loop current when the loop is located at the distance of 10 m and 1 km away from the lightning channel. The engineering model presented in Section II is applied to calculate the incident external field. The channel

base current has the magnitude of 10 kA and the waveform of 0.25/100 μs. (15) is used to determine external source voltage in the wire structure of concern. It is found in Fig. 9 that the induced current is stable in both near-field and far-field zone cases. The induced current in far field zone case is very small, and the waveform is distorted. It has a shape increase in the early time, then slowly increases to its peak value. Two different time steps, i.e., 1.9 ns and 15 ns were adopted in the PEEC simulation. There is no apparent difference in the results. Then $1/20$ of the front time of the channel base current would be adequate for the time step in time-domain simulation.

C) Unstable induced current using the Uman's formula

Unbounded induced current is also observed in the loop when the Uman's formula is applied to calculate the external source voltage in the PEEC model, as seen in Fig. 6(b). In this case, the source voltage is contributed by $\int_0^t I(\tau)d\tau$, $I(t)$ and $\partial I/\partial t$. The corresponding three components of the source voltage in the loop are plotted in Fig. 6(b) as well. It is found that the unbounded induced current is caused by the non-trivial voltage components arising from $\int_0^t I(\tau)d\tau$ and $I(t)$.

Similar to the previous case, the closed-contour integral of electric field can be analytically evaluated. With the identity of $\partial I(z',t')/\partial R = -1/c\,\partial I(z',t')/\partial t'$, the induced source voltage in the loop is obtained, as follows:

$$e_s = \int_C \boldsymbol{E}_{uman}\cdot d\boldsymbol{l} = \iint_S \nabla\times\boldsymbol{E}_{uman}\cdot d\boldsymbol{S}$$
$$= -\frac{1}{4\pi\varepsilon_0}\iint_S \frac{\sin\theta}{c^3 R}\left[\frac{c}{R}\frac{\partial I(z',t')}{\partial t'} + \frac{\partial^2 I(z',t')}{\partial t'^2}\right]\hat{\varphi}\cdot d\boldsymbol{S} \qquad (16)$$

(16) is exactly the same as that for the Jefimenko's formula in (14). Certainly, the induced loop current is theoretically bounded when time goes on.

It is noted that the electric field contributed by $I(t)$ in the Uman's formula is not conservative. When the source voltage of individual segments is numerically evaluated, the retardation effect within the segments cannot be fully considered. Therefore, by ignoring the identity mentioned early the induced source voltage in the loop becomes

$$e_s = \frac{1}{4\pi\varepsilon_0}\iint_S \frac{\sin\theta}{cR^3} I(z', t-\frac{R}{c})\hat{\varphi}\cdot d\boldsymbol{S} \qquad (17)$$

This indicates that the loop current will increase monotonously if the source current has an impulse waveform. An unbound induced current is then observed in the closed loop.

Consider again the same square loop in the near field zone excited by a lightning channel. Simulation of induced loop current was performed using the Uman's formula by varying time step and segment length separately. Fig. 11 shows the induced current with the time step varying from 0.2 ns to 1.0 ns. The segment length was fixed to be 0.1 m or 0.01 m in the simulation. The stable induced current calculated with the improved algorithm (Δl= 0.1 m and Δt = 15 ns) is presented as well for comparison. Apparently, the induced current is not stable in all cases, and tends to be infinite. Nevertheless, a good agreement of the induced current is observed in the early time. The portion of the matched curves increases with decreasing Δt. The induced current is close to the stable result in its tail at Δt=0.2 ns, when Δl is reduced from 0.1 m to 0.01 m. In order to obtain the correct result of the induced current, Δl and Δt must be infinitely small, which are practically infeasible.

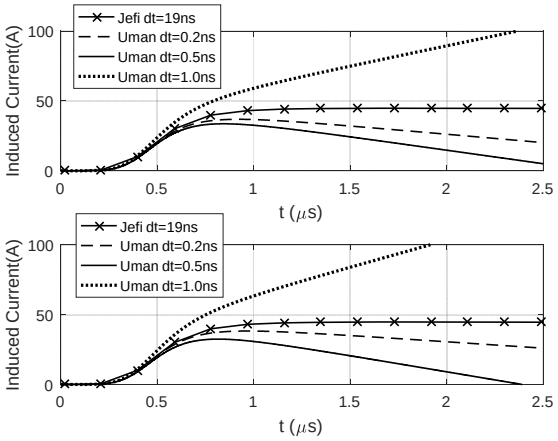

Fig. 10 Unstable loop current in near field zone with different Δl and Δt (top: Δl=0.1 m, bottom: Δl=0.01 m)

It is noted in (17) that the source voltage is inversely proportional to R^3. The source voltage will be very small in the far field region. However, the induced loop current is still unbounded as time goes on. Fig. 11 shows the induced loop current in far field region calculated by the Uman's formula with the time step of 1 ns or 3.8 ns. For comparison, the induced loop current calculated with the Jefimenko's formula is presented in the same figure for reference.

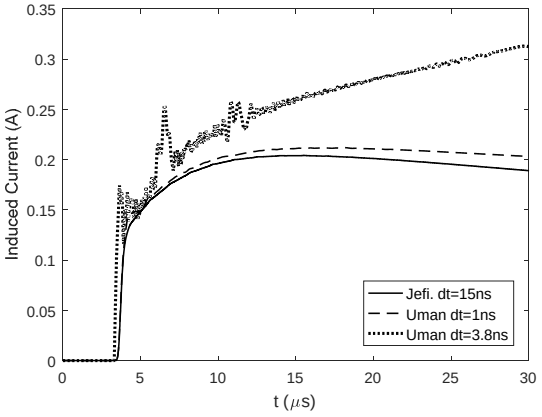

Fig. 11 Unstable loop current in far field zone with the Uman's formula

IV. Evaluation of Induced Transients in a PV Panel under a Distance Lighting Stroke

The proposed PEEC model with the improved algorithm for incident field has been applied to evaluate induced lightning transients in a PV panel. Fig. 12 shows the configuration of the system under investigation. The PV panel has eight PV cells situated above the perfectly conducting ground, and connected in series. Each of these cells is represented with a set of interconnected copper wire segments. These wires have the width of 1.6 mm and the thickness of 0.2 mm. The conductivity

is 3.74x10^7 S/m. Because of the thin thickness, the skin effect is neglected in the wire modelling. Consequently, the resistance of the wires is approximated by the DC resistance, and self-inductance by the DC inductance.

The engineering model presented in (1) is adopted for the lightning current in the channel. The channel base current has a waveform of 0.25/100 μs and an amplitude of 10 kA. The current attenuates exponentially along the channel with attenuating factor $p(z') = e^{-z'/1700}$. The velocity of the return stroke current is assumed to 1/3 of the light speed. The PV panel is situated at the distance of 5 m from the lightning channel.

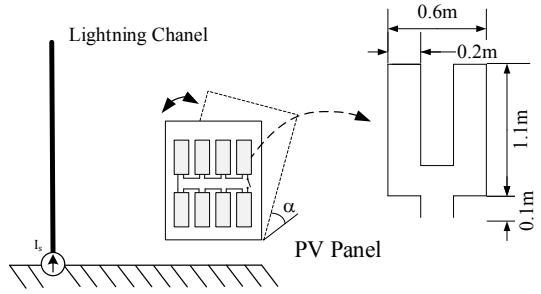

Fig. 12 Configuration of the PV Panel during an indirect lightning strike

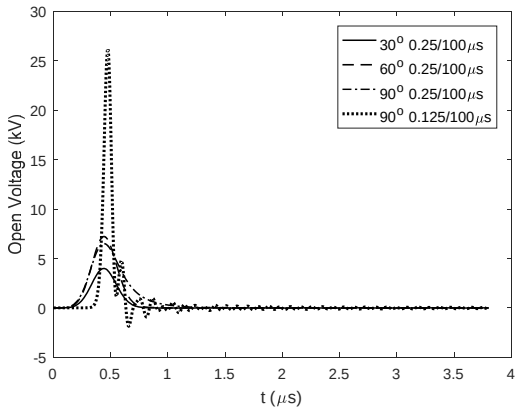

(a) Open voltage from the panel tiled by 30° to 90°

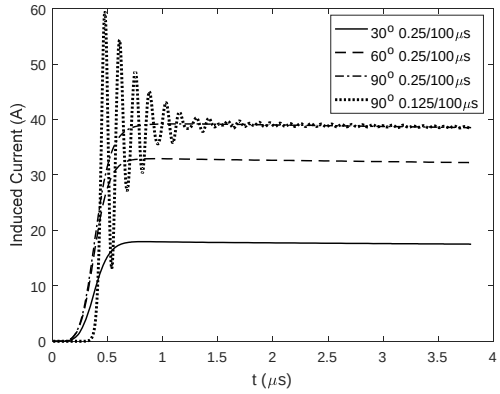

(b) Induced current from 30° to 90° tiled by 30° to 90°

Fig.13 Simulation results of lightning transients on the PV panel

The Jefimenko's formula with the improved algorithm given in (15) was applied to evaluate external incident field sources in the wire segments of the PV panel. In the PEEC model, the wires are divided into a set of segments with the equal length of 0.1 m. The time step was set to be 15 ns for I_s with 0.25 μs front time, and 5 ns for 0.125 μs front time. In the simulation, the induced lightning current in the DC loop of the panel is calculated. The induced lightning voltages in the PV panel is simulated as well when the DC circuit is open.

Fig. 13(a) shows the waveforms of the open voltage when angle α of the PV panel is changed from 30° to 90°. The peak value of open voltage in the 90° panel arrangement is the largest, and reaches 7.5 kV approximately. It is increased to 30 kV when the front time of the current waveform is as short as 0.1 μs. Fig. 13(b) shows the waveform of the induced current. The peak value of the induced current is close to 40 A for the 0.25/100 μs lightning stroke, and reaches 58 A for the 0.125/100 μs lightning stroke. The simulation results indicate that substantially transient voltages will be experienced on the PV panel if it is close to the lighting channel. It is necessary to provide surge protective devices on the DC wires for lightning protection. Lightning induced current, however, is not significant on the PV panels.

IV. Conclusions

This paper presented a time-domain full-wave PEEC model for evaluating transients in a wire structure, which was exposed to an external incident field form a lightning channel. The engineering model of a lightning channel was applied to determine channel current distribution, and the Jefimenko's formula was proposed to calculate external incident field source in the wire structure. Instable current in a closed wire loop was found in the simulation. The investigation revealed that the problem was caused by discretization of electric field in the numerical evaluation of source voltage, and the retardation effect cannot be fully considered in the computation. An improved algorithm for stable incident simulation in a loop structure was proposed, and was validated numerically by the FDTD method. The proposed method was applied to evaluate induced lightning transients in a PV panel. It was also found that the Uman's formula which was widely used for field-to-line coupling calculation was generally incapable of producing stable induced currents in the short-wire loop structure.

Acknowledgment

The work leading to this paper was supported by grants from the Research Grants Council of the HKSAR (Project No. PolyU 152100/18E and 152038/15E).

References

[1] C. D. Taylor, R. S. Sattenvhite and C.W. Harrison, "The response of a terminated two-wire transmission line excited by a nonuniform electromagnetic field," IEEE Trans. on AP, vol. 13, 1965, pp. 987-989

[2] A. K. Agrawal, H. J. Price, and S. H. Gurbaxani, "Transient response of multiconductor transmission lines excited by a nonuniform electromagnetic field," IEEE Trans on EMC, vol. 22, 1980, pp. 119~129

[3] P. Chowdhuri and E.T. B. Gross, "Voltage surges induced on overhead lines by lightning strokes," Proc. of IEE, vol. 114 no. 12, 1967, pp. 1899~1907

[4] P. Chowdhuri, "Lightning induced voltages on multiconductor overhead lines," IEEE Trans. on PWRD, vol. 5 no. 2, 1990, pp. 658~667.

[5] M.A. Uman, D.K. McLain and E. P. Krider, "The electromagnetic radiation from a finite antenna." American Journal of Physics, vol. 43 no. 1, pp. 33-38.

[6] C. A. Nucci, M. Ianoz, and C Mazzetti, “Comparison of two coupling models for lightning-induced overvoltage calculations,” IEEE Trans. on PWRD, vol. 10 no. 1, 1995, pp. 330~339.
[7] V. Cooray, “Calculating lightning-induced overvoltages in power lines: A comparison of two coupling models,” IEEE Trans on EMC, vol. 26 no 3, 1994, pp. 79~182
[8] S. Tkatchenko, F. Rachidi and M. Ianoz, "Electromagnetic field coupling to a line of finite length: Theory and fast iterative solutions in frequency and time domains," IEEE Trans on EMC, vol. 37 no. 4,1995, pp. 509-518
[9] Y P. Yutthagowith, A. Ametani, F. Rachidi, N. Nagaoka & Y. Baba, "Application of a partial element equivalent circuit method to lightning surge analyses." EPSR, vol. 94, 2013, pp. 30-37.
[10] Du, Xinghua Wang and Mingli Chen, “Circuit parameters of vertical wires above a lossy ground in PEEC models”, IEEE Trans. on EMC, vol. 54, no. 4, 2012, pp.871-879
[11] G. Ala and M.L.Di Silvestre. "A simulation model for electromagnetic transients in lightning protection systems." IEEE Trans on EMC, vol. 44 no. 4, 2002, pp. 539-554.
[12] G. Antonini, S. Cristina, and A. Orlandi. "PEEC modeling of lightning protection systems and coupling to coaxial cables." IEEE Trans on EMC vol. 40 no. 4, 1998, pp. 481-491.
[13] Q. B. Zhou and Y. Du, “Using EMTP for evaluation of surge current distribution in metallic gridlike structures,” IEEE Trans. Ind. Appl., vol. 41, no. 4, 2005, pp. 1113–1117
[14] H. Chen, Y. Du and M. Chen, "Lightning transient analysis of radio base stations." IEEE Trans on PWRD, Vol. 33, no. 5, 2018, pp. 2187-2197
[15] Hongcai Chen and Ya-ping Du, “Model of Ferromagnetic steels for lightning transient analysis.” IET Science, Measurement & Technology, Vol. 12 no. 3, 2018, pp. 301-307
[16] S. Tkatchenko, N. Theethayi, Y. Baba, F. Rachii and R. Thottappillil, “On the choice between transmission line and full-wave Maxwell’s equation for transient analysis of buried wires,” IEEE Trans. EMC, vol. 50, no. 2, 2008, pp. 347–357
[17] K. Tanabe, A. Asakawa, M. Sakae, M. Wada, and H. Sugimoto, “Verifying the computational method of transient performance with respect to grounding systems based on the FD–TD method,” IEEJ Trans. Power Energy, vol. 123, no. 3, 2003, pp. 358–367 (in Japanese).
[18] Y. Baba, N. Nagaoka, and A. Ametani, “Modeling of thin wires in a lossy medium for FDTD simulation,” IEEE Trans. Electromagn. Compat., vol. 47, no. 1, 2005, pp. 54–60
[19] M. Akbari, K. Sheshyekani, A. Pirayesh, F. Rachidi, M. Paolone, A. Borghetti, and C.A. Nucci, “Evaluation of lightning electromagnetic fields and their induced voltages on overhead lines considering the frequency dependence of soil electrical parameters,” *IEEE* Trans on EMC, vol. 55 no. 6, 2013, pp. 1210-1219
[20] A. Ruehli, Jan Garrett and Clayton Paul. "Circuit models for 3D structures with incident fields," Procs. of 1993 IEEE International Symposium on EMC. IEEE, 1993. 1993 Intern. Symp. on EMC, 1993, pp. 28-32
[21] K. A. Michalski and D. Zhang, “Electromagnetic scattering and radiation by surfaces of arbitrary shape in layered media, part I: theory,” IEEE trans. on AP, vol. 38 no. 3, 1990, pp. 335-344.
[22] B. Gustavsen and A. Semlyen, "Rational approximation of frequency responses by vector fitting," IEEE Trans. PWRD., vol. 14, no. 3, 1999, pp. 1052–1061
[23] V.A. Rakov and M. A. Uman, "Review and evaluation of lightning return stroke models including some aspects of their application." IEEE trans. on EMC, vol. 40 no. 4, 1998, pp. 403-426.
[24] R. Moini, B. Kordi, G.Z. Rafi and V.A. Rakov, "A new lightning return stroke model based on antenna theory." JGR: Atmospheres, vol. 105 (D24), 2000, pp. 29693-29702.
[25] Xuan-Min Shao, "Generalization of the lightning electromagnetic equations of Uman, McLain, and Krider based on Jefimenko equations." *JGR: Atmospheres,* vol. 121 no. 7, 2016, pp.3363-3371.
[26] R. Rhottappillil and V. Rakov. "Review of three equivalent approaches for computing electromagnetic fields from an extending lightning discharge," *Journal of Lightning Research*1, vol. 1, 2007, pp. 90-110.